

**STATUS OF THE SLC\***

D. P. COUPAL

*Stanford Linear Accelerator Center*

*Stanford University, Stanford, CA 94309 USA*

**ABSTRACT**

This report presents a brief review of the status of the Stanford Linear Collider.

*Presented at the 24th Rencontres de Moriond:  
Electroweak Interactions and Unified Theories,  
Les Arcs, France, March 5-12, 1989.*

---

\* Work supported by Department of Energy contract DE-AC03-76SF00515.



the positron damping ring, joining the remaining positron bunch that will be kicked in the next cycle. In this manner, each positron bunch is damped for two machine cycles.

Electron and positron beams were successfully collided with small beam sizes in Summer 1988. A successful test of the linear collider principle, the integrated luminosity was still too low to produce an  $e^+e^-$  annihilation into a  $Z^0$  boson. This machine's luminosity is given by:

$$L(\text{cm}^{-2} \text{ sec}^{-1}) = \frac{f N^+ N^-}{4\pi \sigma_x \sigma_y},$$

where  $f$  is the machine repetition rate,  $N^+$  and  $N^-$  are the bunch intensities, and  $\sigma_x$  and  $\sigma_y$  are the beam sizes (assuming electron and positron beams are the same size). Table 1 shows typical values for these parameters to date, and the beginning goal for 1989 runs.

**Table I.** SLC luminosity parameters.

Parameter	1988 (Typical)	1989 Startup
$f$ = repetition rate	<b>30</b> Hz	<b>60</b> Hz
$N^- = e^-$ intensity	<b>0.8</b> x $10^{10}$	1.2 x $10^{10}$
$N^+ = e^+$ intensity	<b>0.8</b> x $10^{10}$	1.2 x $10^{10}$
$\sigma_x \times \sigma_y$ = spot size at IP	5 x 3 $\mu\text{m}$	5 x 3 $\mu\text{m}$

The running in 1988 was plagued by reliability problems that limited the efficiency for maintaining these parameters to 1-2%. The parameters for the 1989 startup correspond to a luminosity of  $4.6 \times 10^{27} \text{ cm}^{-2} \text{ sec}^{-1}$ . The visible cross section on the  $Z^0$  peak is 30 nb, corresponding to 12  $Z^0$ s per day at 100% efficiency.

Section 2 describes **the machine progress** and limitations affecting each above-mentioned luminosity parameter. Section 3 discusses the status of the detectors and the understanding of backgrounds in the Mark II detector. The final section looks at future prospects.

## 2. LUMINOSITY

### 2.1 Repetition Rate

The SLC design calls for a repetition rate of 180 Hz. The linac is currently limited to 120 Hz due to power limitations in the linac subboosters. A further rate limit is due to the extraction kickers that kick the beam out of the damping rings to the linac. It was found early on that the kicker for the electron damping ring could not reliably kick out both electron bunches as called for in the mode described above. Until a new kicker is designed, the SLC is run with one electron bunch in the ring and alternate cycles devoted to positron production, thus limiting the rate to 60 Hz.

### 2.2 Beam Intensity

The electrons are provided by a conventional cathode source capable of producing the design intensity ( $7 \times 10^{10}$ ). The positrons are created by dumping a 33 GeV electron bunch

on a tungsten target. The emitted positrons are collected, focused, transported back to the front of the machine, accelerated up to 1.2 GeV and injected into the positron damping ring. Each step involves a loss of intensity. The maximum achieved for the ratio of positrons produced per incident electron is 2.0 in the positron return line, 1.5 into the damping ring and 1.0 at the linac end. Recent improvements (discussed below) should improve this yield.

The damping rings are required to reduce the emittance of the beams sufficiently to achieve the small design spot sizes. The damping time for electrons is 10 msec. Positrons start off with larger emittance and therefore are damped for two machine cycles. Excessive impedance in the damping rings caused the bunch length to be longer than design at bunch intensities above  $2-3 \times 10^{10}$ . Changes installed in the electron ring-to-linac line and planned for the positrons increase the acceptance to correct for this effect.

The linac accelerates the 1.2 GeV bunches from the damping rings up to the full energy (currently at 46.0 GeV). At bunch intensities above  $1.0 \times 10^{10}$  the interaction of the particles within a bunch with other particles or with the accelerating structure becomes important. The head of the bunch leaves behind wakefields that decelerate the particles in the tail. The effect is corrected for by running with the bunch slightly ahead of the RF crest. In addition, transverse oscillations down the linac will cause transverse wakefields which tend to push the tail out to larger amplitude. By the end of the linac, the bunch is significantly distorted. A partial solution to this problem is referred to as BNS<sup>1)</sup> damping. This technique introduces an energy difference between the head and the tail at the beginning of the linac, removing it as the bunch accelerates down the linac. This energy difference destroys any coherent effects between the head and tail-significantly reducing the distortion.

### **2.3 Beam Size at the Interaction Point**

The electron and positron bunches are transported through the arcs to the Final Focus System (FFS). Initial alignment problems with the arcs have been solved and they now operate close to design specifications. Dispersion and s-y coupling in the arcs is small enough to be correctable in the FFS. The beginning of the FFS is designed to accept beam from the arcs and cancel any dispersion or z-y coupling. The beam then goes through the first half of the demagnification, a chromatic correction section, and a final demagnification before reaching the interaction point (IP). After the collision, the beams go half-way out the FFS, where they are kicked out to beam dumps. In the line to the beam dump, an energy spectrometer (described below) measures the energy of each bunch to an accuracy of 25 MeV.

The IP has a number of diagnostics for measuring and monitoring beam sizes and positions. Two *wire flippers* move sets of thin horizontal and vertical wires near the IP. The beam can then be steered to either a 30, 7 or 4  $\mu\text{m}$  wire. Beams striking the wire can be detected by two

methods: (a) a current will flow on the wire due to secondary emission, and (b) bremsstrahlung photons are emitted along the beam direction. Monitoring either of these signals as the beam is scanned across the wire gives a measure of the beam size. The bremsstrahlung photons are detected using a converter and Čerenkov counter designed to look at *beamstrahlung*, the synchrotron photons from beam particles bending in the magnetic field of the other bunch. Figure 2 shows an example of the beam spot profiles obtained from these signals.

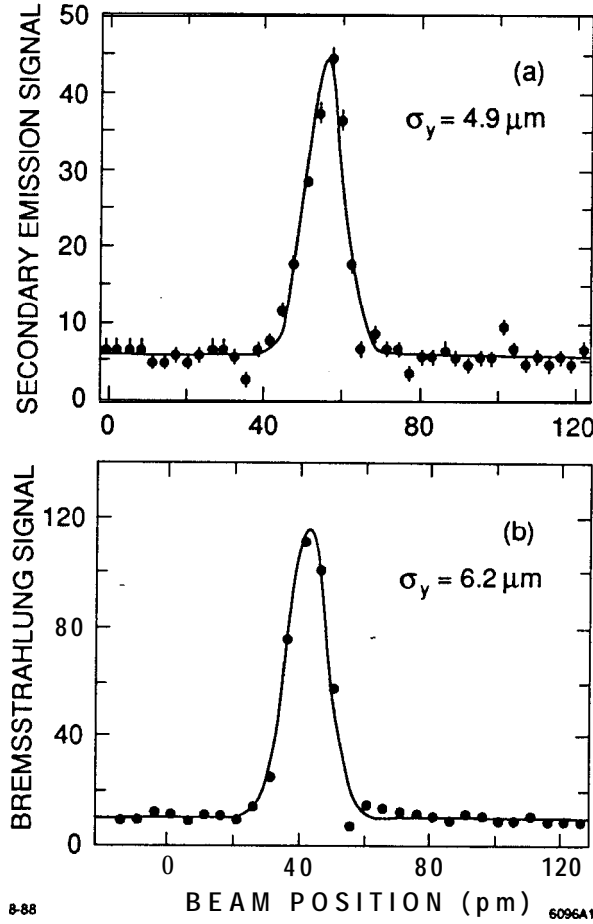


Figure 2: Examples of beam spot profiles obtained from the secondary emission and bremsstrahlung signals on a  $7 \mu\text{m}$  wire.

The beam size at the IP is given by:

$$\sigma_{IP}^2 = \sigma_{MIN}^2 + \sigma_{\theta}^2 \times A f^2 + \eta^2 \times \left(\frac{\delta E}{E}\right)^2 + \sigma_{xy}^2 + \text{higher-order terms} ,$$

where  $\sigma_{MIN}$  (the minimum spot size) and  $\sigma_{\theta}$  (the angular spread at the IP) are determined from the beam emittance and the value of the beta function at the IP ( $\beta^*$ ),  $A_j$  is the shift in the focal point,  $\eta$  is the dispersion at the IP,  $\delta E/E$  is the energy spread, and  $\sigma_{xy}$  is the contribution from x-y coupling in the beam. The only significant higher-order terms are the second-order, which are cancelled in the chromatic correction section.

The focal point can be set at the IP simply by varying the focal distance and finding the value that gives minimum spot size. A scan example is shown in Fig. 3. Similar scans can be

used to reduce the contribution of other terms: finding the minimum spot size versus strength of skew quadrupoles in the FFS eliminates contributions from  $x$ - $y$  coupling, and purposely introducing dispersion in the FFS can be used to cancel dispersion at the IP. With the other contributions removed, a final waist scan then yields  $\sigma_{MIN}$  and  $\sigma_{\theta}$ , therefore measuring emittance and  $\beta^*$ . The emittances measured in this manner agree with values measured at the end of the linac after correcting for the expected emittance growth in the arcs.

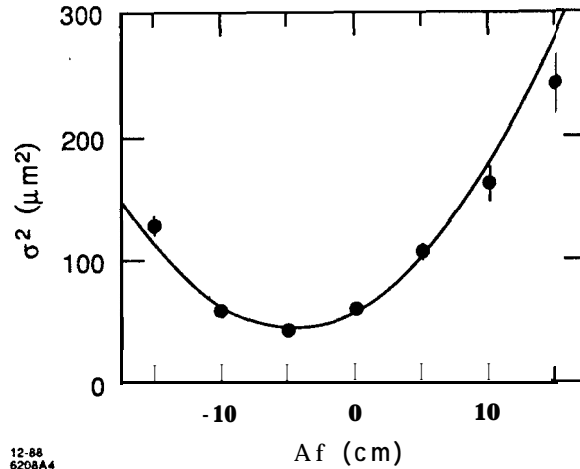


Figure 3: Typical waist scan, measuring spot size at the IP vs. waist position.

## 2.4 Colliding the Beams

When the beams are tuned to the minimum spot size using the wire flippers, each beam is steered to the same reference point relative to a given wire. The wire flipper is then removed and beam-beam deflection brings the beams into collision. Beam-beam deflection is simply the deflection of one beam by the electric field of the other. Figure 4(a) shows the beam deflection angle resulting as one beam is scanned across the other. Figure 4(b) shows the beamstrahlung signal for such a scan. The small dip at the center is due to the field's going to zero at the center of the bunch. An automated procedure that scans one beam in  $x$  and  $y$  is performed every 10 to 15 minutes to maintain the beams in collision to an accuracy of order  $1 \mu\text{m}$ .

## 3. DETECTORS AND BACKGROUNDS

### 3.1 Status of Detectors

The Mark II was moved onto the beam line in October 1987. Shown in Fig. 5, it consists principally of a central tracking chamber in a 4.75 kG magnetic field surrounded by electromagnetic calorimetry and a muon identifier consisting of iron walls and proportional tubes. The barrel calorimeter, is lead/liquid argon and the endcap is lead/proportional tube. A time-of-flight system and  $dE/dx$  in the central drift chamber provide particle identification. The Mark II has a vertex drift chamber ready to be installed and a silicon microstrip detector that will be ready by the end of the Summer of 1989. At the moment, the wire flipper at

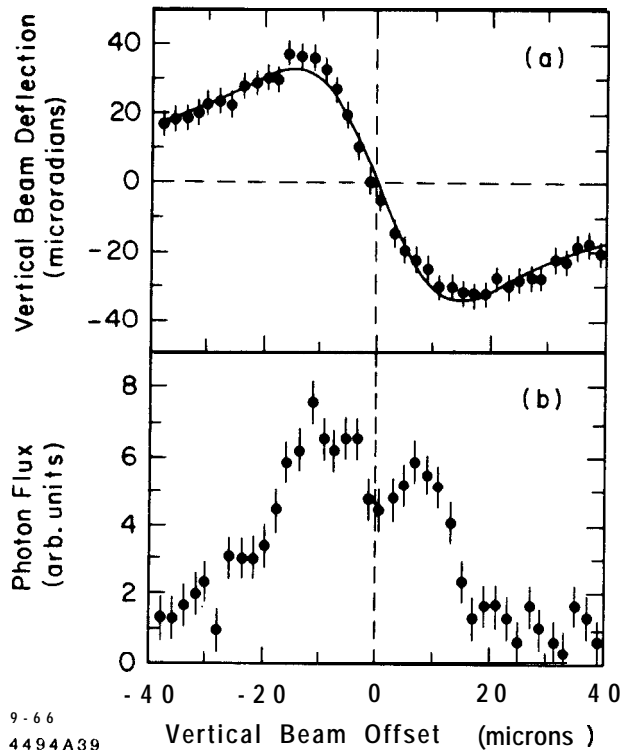
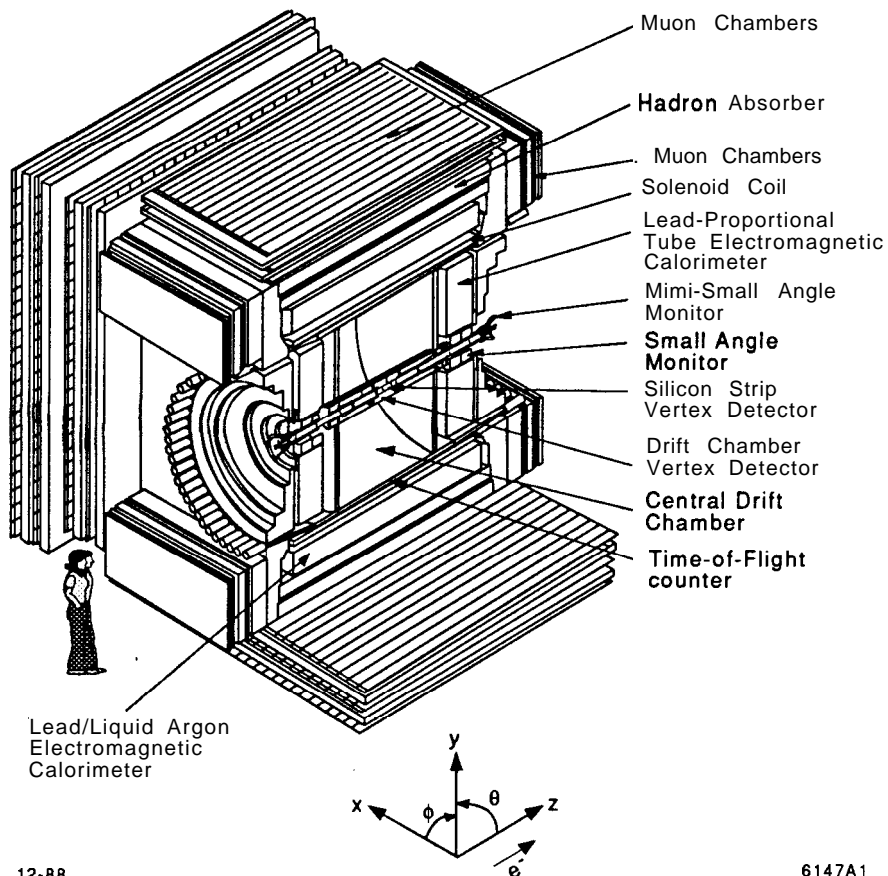


Figure 4: The signals from beam-beam dejection. The angular deflection of one beam as the other is scanned across it is shown in (a). The resulting beamstrahlung signal is shown in (b).

### MARK II AT SLC



12-88

6147A1

Figure 5: The Mark II detector at the SLC.

the IP precludes the installation of either detector. It is hoped that tuning with beam-beam deflection will make it possible to remove the wire flipper from the IP.

The larger SLD detector **is** currently under construction and will eventually replace the Mark II. This detector has a CCD microvertex detector, a central drift chamber in a 6 kG magnetic field, electromagnetic and hadronic calorimetry, and particle identification using a ring-imaging Čerenkov detector. The scheduled completion date of the SLD is February 1990.

Currently integrated into the Mark II readout, the energy spectrometers in front of the beam dumps provide  $e^-$  and  $e^+$  energy measurements for each machine pulse. The spectrometer, shown schematically in Fig. 6, measures the separation of two synchrotron stripes on a phosphor screen to determine the energy. The current estimate on the accuracy of the measurement **is** 25 MeV for each beam.

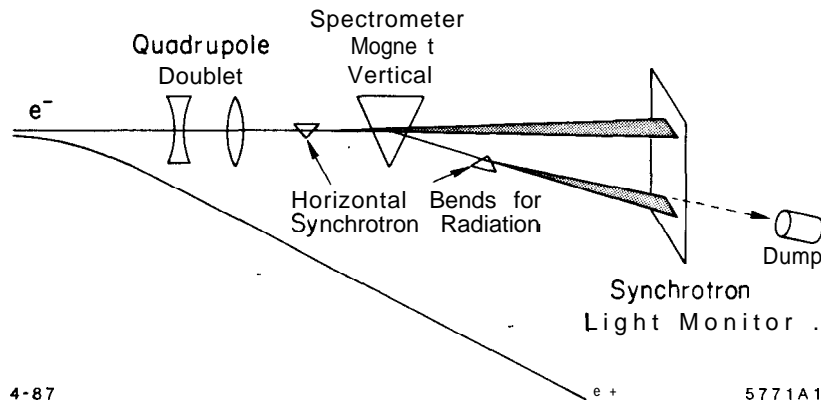


Figure 6: Schematic drawing of the SLC energy spectrometer.

### 3.2 Backgrounds

In spite of steps taken in the linac to reduce the tails on the beam, collimation is still necessary to produce a beam at the IP free of off-energy or off-axis tails. To this end, a set of adjustable collimators at the beginning and reverse bend point of the arc provide primary beam collimation. Additional collimators in the arcs and FFS provide the secondary collimation necessary to **remove** the spray of particles generated by the primary collimators. An additional set of primary collimators is being designed for use in the last linac sector.

The Mark II has identified four principal sources of background in the detector:

1. **Tunnel Shine.** Off-energy or off-axis beam particles strike the beampipe or collimators upstream of the detector. Most products of the resulting shower are absorbed in the beampipe and magnet elements; however, many low-energy photons can scatter out into the beam tunnel, travel down the tunnel and hit the detector. This background shows up as hits in detector elements not shielded from the outside. The solution to this background was to add shielding at the end of the tunnel and shield exposed parts of the detector.

2. Muons. A muon pair is produced for every  $2 \times 10^4$  beam particles stopped in a collimator. For the secondary collimators in the FFS, the probability that a muon hits the detector varies from 2% to 100%, depending on its origin. A loss of  $2 \times 10^4$  represents only one part in  $10^6$  of the beam—thus, effective use of these collimators requires taking some steps to eliminate these muons. The solution was to install large toroidal magnets on and beside the beamline to deflect the muons away from the detector. These toroids provide a factor of 5 to 50 reduction in the number of muons hitting the detector, depending on the origin.
3. Electromagnetic *Showers*. Occasionally, a stray beam or secondary particle will strike the beampipe or a synchrotron mask near the detector. The resulting shower sends large amounts of electromagnetic energy into the detector, showing up in the Mark II low-angle calorimetry. Careful collimation removes this background to insure that no stray particles come close to the detector. The toroids help by allowing tighter collimation in the FFS.

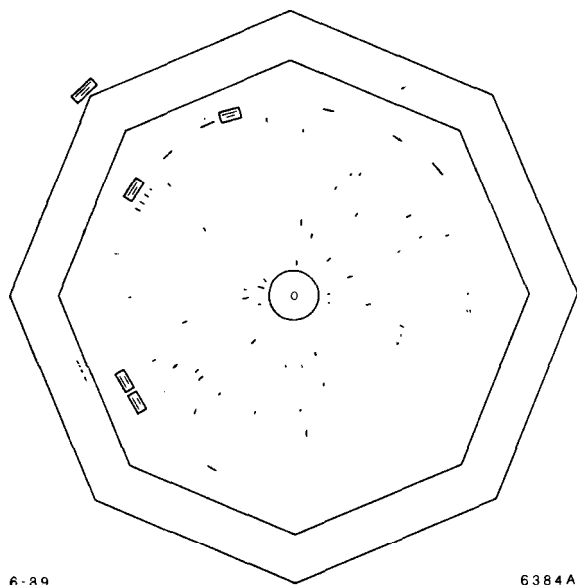


Figure 7: The central detector of the Mark II triggered on a random beam crossing.

4. *Low-Energy Photons in the Detector*. Figure 7 shows the Mark II central detector triggered on a random beam crossing with most of the above backgrounds removed. A number of background hits are observed on the wires of the central drift chamber. An example of the pulses observed on the wires is shown in Fig. 8. The spectrum of energy deposition in the drift chamber gas is consistent with photons in the energy range 10–100 keV. A probable source of these photons is synchrotron radiation from the final quadrupoles being scattered into the detector. The Mark II has masking in and around the beampipe to protect against most of this radiation. However, if the beam is larger than design in the final quadrupole (for example, if the emittance is larger than design) or the masking is not aligned properly, then radiation could scatter into the detector. To date, this background has not been a serious problem, but the beam optics has been set to a  $\beta^*$  of two to four

times design, therefore a smaller beam in the final quadrapoles. Future running at smaller  $\beta^*$  and higher intensities will determine the extent to which this background is a problem.

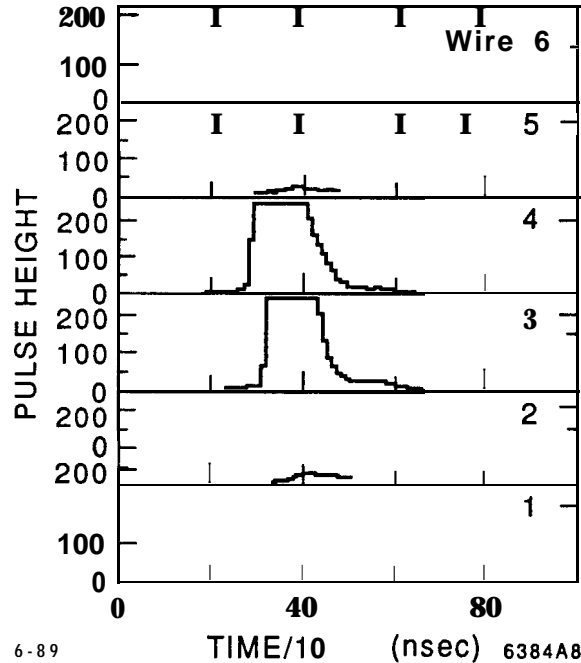


Figure 8: The digitized pulse height vs. time from a photon interaction in one of the six-wire cells of the central drift chamber.

Efforts to isolate and reduce backgrounds in the Mark II detector have been generally successful. Pushing to higher intensities and smaller spots may present new problems.

#### 4. FUTURE PROSPECTS

Although a successful test of the principle of colliding linear accelerators, the SLC is still well below its design luminosity. A number of short-term and long-term improvements are planned to bring the SLC closer to its design goal.

Short-term improvements include:

- *Sector 30 collimators.* These eight pairs of jaws will enable one to collimate electron and positron beams in x and y at two different betatron phases.
- *Positron yield.* An energy compressor at the input to the positron damping ring and improved acceptance of the extracted beam should improve positron yields.
- *Wireless tuning.* Developing procedures for spot size tuning using beam-beam deflection is required for high currents because the wires cannot withstand currents above  $1.5 \times 10^{10}$ .
- *Reliability.* Numerous changes in hardware and software have been made to increase the reliability and reproducibility of the machine components.

Longer-term projects include:

- *New kicker design.* The current kicker design is unable to kick both electron bunches out of the electron damping ring. This problem limits the machine to single bunches in the ring and therefore a repetition rate of 60 Hz.
- *Superconducting final quadrupoles.* Planned for use with the SLD detector, this addition will reduce the beam size to 1.5  $\mu\text{m}$ .
- *Polarization.* Installation of some polarization components is due to begin in late 1989.<sup>2)</sup>

The prospects for physics from the upcoming run is a function of the integrated luminosity, which is difficult to predict. It depends on the effectiveness of the improvements outlined above and the machine reliability. One of the first measurements one would 'want to make is the  $Z^0$  mass and width. If one assumes a luminosity corresponding to the 1989 startup in Table 1 and an efficiency of 30%, it is not unreasonable to expect  $10 \text{ nb}^{-1}$  by the end of the Summer. This luminosity corresponds to about 300  $Z$ s on the peak of the resonance. Such a luminosity taken at several energies around the  $Z$  peak would yield mass and width errors of:

$$\Delta M_Z \approx 150 \text{ MeV}$$

$$\Delta \Gamma_Z \approx 300 \text{ MeV} .$$

A successful test of the linear collider principle, the SLC is now in a position to prove itself as a physics tool. The upcoming run of the SLC presents the first opportunity to study in detail the physics of the  $Z^0$  boson.

## ACKNOWLEDGEMENTS

This status report drew heavily on a previous report by D. Burke<sup>3)</sup>; I thank him for use of a 'preliminary version. I also appreciate the help of John Seeman and Lenny Rivkin in preparing this report.

## REFERENCES

1. V. Balakin, A. Novokhatsky, and V. Smirnov, *Proc. of the 12th Int. Conf. on High Energy Accel.*, Fermilab, 1983; K. Bane, SLAC/AP-69 (1988).
2. See R. Prepost, these proceedings.
3. D. L. Burke, SLAC-PUB-4851 (1989), to be published in *Proc. of the Mtg. of the Div. of Particles and Fields of the APS*, Storrs, CT (1988).